Int J Adv Manuf Technol (2018) 94:3875–3887
DOI 10.1007/s00170-017-1088-1

ORIGINAL ARTICLE

Coolant strategy influence on tool life and surface roughness when machining ADI

A. Eltaggaz[1] · P. Zawada[1] · H. A. Hegab[2] · I. Deiab[1] · H. A. Kishawy[2]

Received: 17 April 2017 / Accepted: 12 September 2017 / Published online: 26 September 2017

Abstract Austempered ductile iron alloys (ADI) are an interesting class of materials because of their unique microstructure and mechanical properties. When subjected to austempering treatment, ductile iron transforms to a microstructure consisting of ferrite and stabilized austenite rather than ferrite and carbide as in austempered steels. Because of the presence of stabilized austenite, austempered ductile iron (ADI) exhibits an excellent combination of strength and ductility together with good fatigue and wear properties. Accordingly, there is a growing interest in using ADI in several applications due to its mechanical properties. However, as with difficult-to-cut materials, the machinability rating of ADI is low and there is still a need to understand the impact of the cutting process parameters. Machinability of a material depends not only on its properties and microstructure, but also on the proper selection and control of process variables. The current work is focused on performing a machinability analysis of ADI in order to understand the effect of the cutting process parameters on the machined surface quality and tool life. It also studies the effect of different coolant strategies. Thus, the motivation of this study is to develop a better understanding of the influence of cutting parameters and cooling strategy to be able to machine ADI directly with acceptable tool life and cycle time. The design of experiments technique and response surface methodology is employed to analyze and model the measured responses. In addition, the cutting tool wear mechanisms are identified and discussed.

Keywords Machinability · ADI · Cooling strategies · Tool wear · Modeling · Design of experiments

1 Introduction

Machinability rating of a material is an indication of the difficulty or ease with which it can be machined [1]. It can be assessed by the magnitude of cutting forces, cutting parameters, material removal rate, tool life, and surface roughness [2]. From machining viewpoint, when cutting any material, its properties should be taken into account. Such properties include high hardness, toughness, low thermal conductivity, and high strength-to-weight ratio which negatively influence the machinability of material. Materials are hence termed difficult-to-cut materials [3]. Several studies focused on machining difficult-to-cut materials as they are associated with low productivity and high machining cost due to the excessive heat generation, difficulties in chip formation, and heat dissipation at the cutting zone in the presence of high material hardness and strength. The main problems during machining difficult-to-cut materials are short tool life, poor surface integrity, and longer cycle time [4].

Austempered ductile iron (ADI) is an example of difficult-to-cut materials. ADI is a cast iron that is heat-treated providing the designer with high strength-to-weight ratios at a competitive price in comparison to steel. Recently, ADI has attracted research attention due to remarkable properties such as wear resistance, tensile strength (1000–1500 MPa), elongation (3–15%), and fatigue strength [5, 6]. Mechanical properties of ADI can be attributed to the high presence of carbon austenite in its ausferritic matrix (ferrite+ carbon enriched

✉ I. Deiab
ideiab@uoguelph.ca

[1] Advanced Manufacturing Lab, School of Engineering, University of Guelph, Guelph, Ontario, Canada

[2] Machining Research Lab, Faculty of Engineering and Applied Science, UOIT, Oshawa, Ontario, Canada

Table 1 ASTM 897 Property of ADIs [12]

Grade	Tensile strength (MPa/Ksi)	Yield strength (MPa/Ksi)	Elong. (%)	Impact energy (J/lb.-ft)	Hardness (BHN)
1	850/125	550/80	10	100/75	260–321
2	1050/150	700/100	7	80/60	302/363
3	1200/175	850/125	4	60/45	341–444
4	1400/200	1100/155	1	35/25	366/477
5	1600/230	1300/185	N/A	N/A	444–555

austenite) formed after the austempering treatment. Furthermore, some researchers reported that alloying elements added during casting, austenitizing, and austempering temperatures contribute to the variation ADI's mechanical properties [7–9]. ADI components offer a high level of properties over other materials. Table 1 presents the ASTM standard properties of ADI. The table classifies ADI to different grades based on their properties. It can be seen from this table, that all grades have improved strength in comparison to conventional ductile iron. ADI grades are based on the content of the alloying elements added and the selection of both heat treatment temperature and time [5, 10, 11].

On one hand, grades 1, 2, and 3 are assumed the structural grades of ADI; they are often used for applications that require high strength and toughness while keeping a reasonable impact resistance and ductility. These grades are commonly used in manufacturing automotive parts such as suspension components, linkages, crankshafts, and many other dynamic applications. On the other hand, grades 4 and 5 excel in wear and abrasion resistance due to their high hardness. Grades 4 and 5 are used in the replacement of white irons and hardened steels. These grades are commonly utilized to fabricate some constructions and agriculture equipment such as diggers, rollers, and wheels [10]. However, machining grades 4 and 5 is typically accomplished prior to heat treatment due to their extreme hardness.

As seen in Table 1, the hardness of ADI is relatively high which would pose a challenge for any machining process. Despite the hardness of the softer grades of ADI at a value of 300–350 BHN, 40% of the ADI matrix structure is retained austenite. In practice, the austenite phase rapidly transforms to the martensite phase when ADI is subjected to strains, thus contributing to the high hardness [13, 14]. Therefore, these phenomena decrease the ADI machinability in comparison to steel which has the same hardness. Enhancing ADI machinability is crucial due to its increased applications for automotive parts and agricultural rotary machines. Most of ADI machining is done under dry conditions considering the graphite in ADI acts as a good lubricant due to its small coefficient of friction. This results in a longer tool life and reduction the tool wear.

Okazaki et al. [15] reported that the γ-pool (a large amount of austenite which is created on the boundary of the eutectic cell) average area in ADI structure affects the tool wear in drilling. The flank wear of the drill is reduced with the decrease in γ-pool average area and hence, it is significant to reduce the γ-pool in order to improve the machinability. This can be done by re-heating the ductile iron over the martensitic temperature during the tempering process. The double tempering of ductile iron provides a good opportunity for austenite to transform [16]. The results also pointed out that ADI tool wear phenomenon is characterized by extreme crater wear located close to the cutting edge which destabilizes the cutting edge and leads to fracture of the crater lip. The unusual combination of abrasive and adhesive wear mechanisms is due to the special ausferrite microstructure of ADI [15].

Polishetty et al. [17] studied the wear characteristics of ultra-hard cutting tools when machining ADI and its effect on machinability. Turning tests of ADI (ASTMGrade3) using PCBN and ceramics tools were conducted using both roughing and finishing cutting conditions. For roughing, a constant cutting speed (425 m/min) and depth of cut (2 mm) combined with variable feed rates of 0.1, 0.2, 0.3, and 0.4 mm/rev were selected. For finishing, a constant cutting speed (700 m/min) and depth of cut (0.5 mm) combined with variable feed rates of 0.1, 0.2, 0.3, and 0.4 mm/rev were used. Tool wear evaluation, surface roughness, and cutting force were used to compare different cutting inserts performance. The results indicated that when machining ADI material, inserts having high toughness and efficient thermal conductivity are

Table 2 Assignment of levels to cutting process variables

		Symbol	Level 1	Level 2	Level 3	Level 4
Cutting process variables	Feed rate (mm/rev)	A	0.2	0.3	–	–
	Cutting speed (m/min)	B	120	180	240	–
	Lubrication strategy	C	Dry	Flood	MQL	MQL with nanofluid

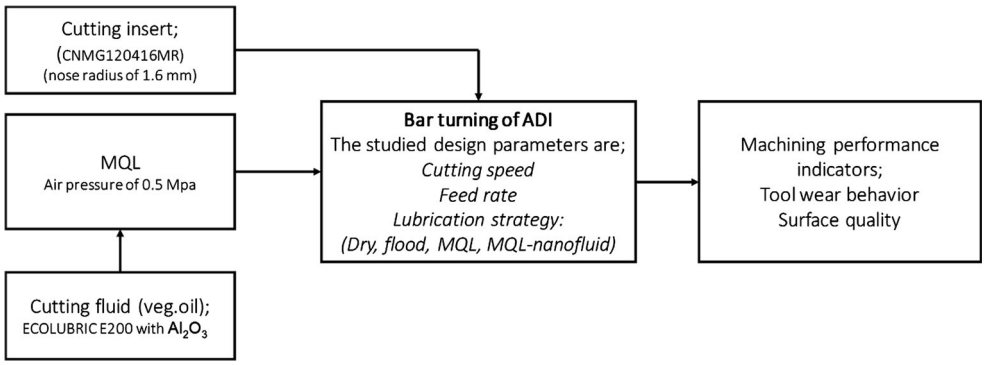

Fig. 1 Experimental setup schematic

appropriate selection. Reduction in cutting forces was observed in finish machining due to thermo-softening effect in the shearing zone.

Different studies have focused on employing and modeling new techniques to improve the difficult-to-cut materials machinability [18–20]. Rotary tools were utilized in machining to reduce the induced wear since a short segment of cutting edge is only engaged with the workpiece [18]. Furthermore, a force model is developed for self-propelled rotary and good agreement has been noticed between the predicted and experimental results using a varied range of cutting conditions [19]. Also, Kishawy [20] provided a comprehensive study on the effects of various cutting variables on the generated cutting temperature when cutting difficult-to-cut material.

Additionally, Davim and Figueira [21] employed standard orthogonal array and analysis of variance (ANOVA) in order to study the surface quality when hard turning of cold work tool steel (D2) with ceramic tools. It was found that average surface roughness of 0.8 μm could be achieved by considering appropriate machining parameters on hard turning without

Table 3 L24OA experimental result

Run #	Lubrication technique	Feed rate (mm/rev)	Cutting speed (m/min)	Tool life (min)	Average surface roughness (μm)
1	Dry	0.2	120	2.72	0.952
2	Dry	0.2	180	1.98	0.895
3	Dry	0.2	240	1.2	0.857
4	Dry	0.3	120	2.29	1.614
5	Dry	0.3	180	1.48	1.634
6	Dry	0.3	240	0.88	1.769
7	Flood	0.2	120	3.41	1.257
8	Flood	0.2	180	2.31	1.016
9	Flood	0.2	240	2.19	1.761
10	Flood	0.3	120	3.45	1.468
11	Flood	0.3	180	2.3	1.126
12	Flood	0.3	240	1.04	1.053
13	MQL	0.2	120	3.01	0.695
14	MQL	0.2	180	2.27	1.005
15	MQL	0.2	240	1.7	0.735
16	MQL	0.3	120	2.27	1.775
17	MQL	0.3	180	1.86	1.564
18	MQL	0.3	240	1.4	1.69
19	Nanofluid	0.2	120	3.55	0.85
20	Nanofluid	0.2	180	2.68	0.88
21	Nanofluid	0.2	240	2.3	0.625
22	Nanofluid	0.3	120	2.85	1.467
23	Nanofluid	0.3	180	2.42	1.98
24	Nanofluid	0.3	240	1.2	1.55

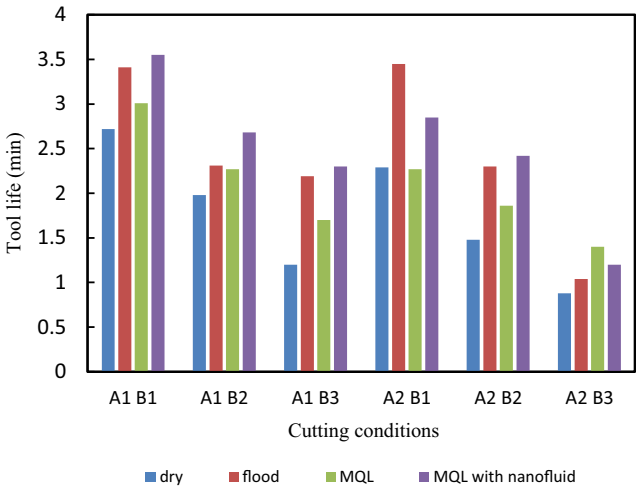

Fig. 2 Tool life results

any need of extra grinding operations. Gaitonde et al. [22] applied the response surface methodology (RSM) in order to investigate the effect of different cutting parameters on machinability of high chromium AISI D2 cold work tool steel using wiper ceramic tools. RSM provided appropriate details about the optimal cutting parameter levels for minimum surface roughness and flank tool wear. Also, Gaitonde et al. [23] investigated the effects of different cutting tools when hard turning of AISI D2 cold work tool steel using full factorial design experimentations. It has been found that wiper ceramic inserts show better results in terms of surface roughness and tool wear; however, CC650 conventional inserts offer better results in reducing the power consumption.

Ahmet et al. [24] studied the influence of depth of cut and cutting speed on machinability of ADI. They evaluated ADI machinability by measuring surface roughness, cutting forces, and flank wear. The response surface methodology (RSM) approach was used to study the influences of machining factors on ADI machinability. The results suggest that depth of cut has insignificant influence on the surface roughness but it has a significant influence in terms of cutting forces. Seker et al. [25] studied the effect of ADI microstructure and properties on its machinability in terms of cutting forces and surface roughness. Six different specimens were prepared under different austempering times with the addition of Cu and Ni at various contents. Cutting tests showed that austempering heat treatment resulted in considerable improvement in the machined surface quality and 20% increase in cutting forces when compared to as-cast specimens.

Klocke et al. [26] developed a finite element simulation for machining of ADI to optimize cutting insert geometry. When machining ADI, discontinuous chip formation in combination with the strong tendency of hardening of the austenitic-ferritic matrix was identified as a major wear mechanism. This resulted in extreme peaks of cutting forces and high specific mechanical load on the insert edge. Using the developed tool, the effects of variation in tool geometry on the alternating tool load were investigated and the optimum geometries were experimentally validated. Tool life was increased by 70% in dry turning and by 100% in wet conditions. Klock et al. [27] revealed that a better understanding of the interactions of microstructure, chip formation, machining properties, cutting material, and wear mechanisms is crucial for optimizing the cutting parameters when machining ADI. Authors stated extreme crater wear located near to the cutting edge is the aspect of tool wear of ADI. In order to understand this wear phenomenon, a more understanding of the machinability behavior of ADI is required. A combination of adhesive and abrasive wear mechanism is also detected in this study which caused by the special austenitic-ferritic microstructure of ADI.

The main aim of this research is to develop a better understanding of the influence of cutting parameters linked with machining ADI and cooling strategies to be able to machine ADI directly with acceptable tool life and cycle time.

2 Methodology

In this paper, a well-defined test matrix was developed to evaluate the process outputs such as machined surface quality and cutting tool performance when machining ADI grade 2 under different machining parameters (i.e., feed, speed, and coolant strategy). The data collected from these experiments were analyzed to gain a better understanding of the impact of changing parameters on different process outputs such as tool wear, tool life, and surface roughness. In the context of this work, nanofluids refer to a cooling-lubrication system consisting of (a) gamma Al_2O_3 nanoparticles and (b) base fluid. The nanoparticles are mixed with base fluid, rapeseed oil, using volume fraction of 4.0% as suggested in the literature [28–33]. In order to ensure the homogeneity of the nanofluid, a magnetic shaker was used to shake the nanofluid

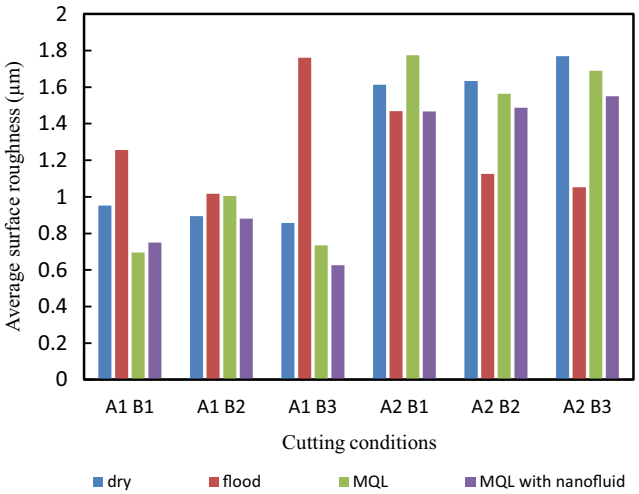

Fig. 3 Average surface roughness results

Table 4 ANOVA results for average surface roughness (Ra)

Sources	Statistical summation	Degree of freedom	Variance	*F* calculated	Results
Lubrication technique	0.099	3		Pooled factor	
Feed rate (*f*)	1.909	1		Pooled factor	
Cutting speed (*v*)	0.013	2		Pooled factor	
Lubrication*v	0.250	6		Pooled factor	
Lubrication*f	2.981	3	0.99	200	Significant at 99% confidence level
v*f	1.951	2		Pooled factor	
Error	0.099	20	0.00495	Pooled factor	
Total	1.909	23		Pooled factor	

coolant before each cutting pass. The nanofluid efficiency as a coolant relative to classical coolant is assessed. Tool wear progress and mechanisms are examined and evaluated by optical and scanning electron microscopy (SEM). The effects of these strategies on the surface quality are also studied.

3 Experimental setup and design

In this work, austempered ductile iron (ADI) grade 2 is used as the workpiece. The mechanical properties of ADI grade 2 are shown in Table 1. Coated carbide tool (CNMG120416MR) with 1.6 mm nose radius is used for the cutting tests. Four different coolant strategies are utilized in this study, namely, dry machining, flood cooling, MQL with vegetable oil, and MQL with nanofluid. Al_2O_3 nanoparticles, are dispersed into MQL 4% as suggested in the literature [28–33]. Turning experiments are conducted at a depth of cut (DOC) of 0.5 mm and length of cut of 50 mm, while different levels of cutting speeds and feeds are utilized as shown in Table 2. The 24 cutting experiments are conducted using L24 mixed orthogonal array based on the design of experiments technique. Each run is performed twice to evaluate the results replicability. The cooling strategies are evaluated at different levels of high and low cutting speed and feed, which have been chosen based on the ranges of recommended cutting parameters by the insert manufacturer.

The administration of both MQL and nanofluid cooling is provided using an external booster pump, mixed with a compressed air. The vegetable oil used is rapeseed oil, ECOLUBRIC E200. The oil is confirmed as friendly environmental and has a biodegradability of 90% in 28 days. The machining tests were conducted on a HASS CNC-lathe machine. A Mitutoyo surface roughness profiler is used to measure the surface roughness values. In addition, a digital camera mounted on a tool maker's optical microscope is used for tool wear measurement. FEI INSPECT S50 SEM is employed to take SEM images along with XT microscope server program for insert images analysis. The experimental setup schematic is presented in Fig. 1.

4 Results and discussions

The findings of this study are discussed in this section. A maximum flank tool wear of (VB = 0.5 mm) is used as the tool life criteria. The tool life and average surface roughness results are shown in Table 3. The test matrix is developed with the aim of relating the influence of input parameters to all measured responses.

The best performance of the cutting tool in terms of tool life is recorded at cutting speed of 120 m/min, feed rate of 0.2 mm/rev using MQL nanofluid technique as shown Fig. 2. The 4% volume nanofluid coolant showed the highest tool life in comparison to the other employed techniques. The MQL-nanofluid shows improvement percentages in tool life of 19.4, 4.1, and 30.5% in comparison with tests performed at same cutting conditions using MQL, flood, and dry techniques, respectively. Flood coolant shows better results only at cutting speed of 120 m/min and feed rate of 0.3 mm/rev; however, it is still not an environmentally friendly technique

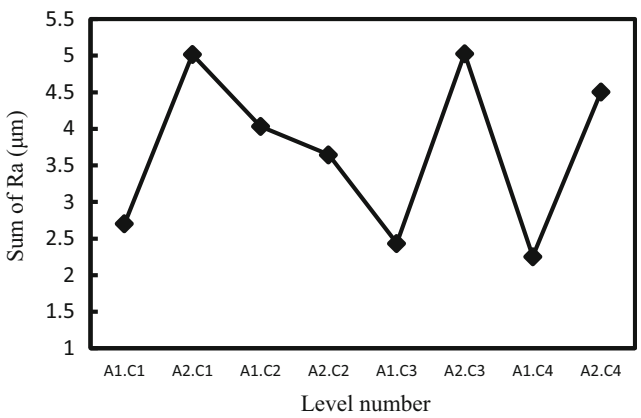

Fig. 4 The interaction effect between the lubrication strategy and feed rate for the average surface roughness results

Table 5 ANOVA results for tool life results

Sources	Statistical summation	Degree of freedom	Variance	*F* calculated	Results
Lubrication technique	2.164	3		Pooled factor	
Feed rate (*f*)	1.44	1		Pooled factor	
Cutting speed (*v*)	8.48	2		Pooled factor	
Lubrication*v	10.96	6	1.82	14	Significant at 99% confidence level
Lubrication*f	3.69	3		Pooled factor	
v*f	10.10	2		Pooled factor	
Error	2.21	17	0.13	Pooled factor	
Total	13.18	23		Pooled factor	

while MQL-nanofluid is considered as a sustainable technique as it offers an optimal amount of cutting fluid (environmentally friendly system).

Several studies have shown that the use of MQL results in a better surface than dry machining [34–36] which is relatively consistent with that shown in Fig. 3. The MQL also reduces the cutting temperature, cutting forces, tool wear, and friction coefficient in comparison with dry machining. However, the average surface roughness results suggest that the nanofluid appears to be the best choice when operating at a low feed rate; however, the flood coolant appears to provide relatively better results at higher feed rate values.

Additionally, from Figs. 2 and 3, it can be seen that the shorter tool life and the coarser surface finish are obtained when machining ADI at the highest levels of cutting speed and feed (240 m/min and 0.3 mm/rev) for all employed cooling strategies. Thus, compared to the tests performed using lowest levels of cutting speed and feed rate, the tool life values are decreased by 65, 64, 52, and 63% for dry, flood, MQL, and nanofluid, respectively. Consequently, the surface roughness values are increased by 46, 58, and 51% for dry machining, MQL, and nanofluid, respectively under using the highest levels for both cutting speed and feed rate.

Generally, the appropriate chip breaking features and potential low machining temperatures make cast iron materials proper for machining processes, which are conducted under dry condition. However, Klocke et al. [37] pointed out that in many cases the use of cooling strategy is significant in machining ADI and is associated with some substantial benefits which agrees with the results shown in Fig. 2. The flood coolant has an advantage in terms of chip clearing as the high liquid pressure at the cutting zone helps to move the chips away of the cutting tool, thereby avoiding the recut chips phenomenon and eliminating a crater wear which could damage the machined surface and dull the cutting tool faster.

Many researchers [38–40] have reported that adding nanoparticles into a base fluid offers a reasonable reduction in friction and greatly enhances its wettability. Different mechanisms were discovered to clarify the enhancement in lubricity of nanofluids, including effect of ball bearing, tribo-film formation, mending, and polishing effects [38]. In this work, the nanofluid enhancements can be attributed to the thermal conductivity improvements of the MQL due to the proper dispersion of Al_2O_3 nanoparticles into the base cutting fluid which enhances the resultant thermal conductivity value in comparison with the base lubricants because of the remarkable properties of the added Al_2O_3 nanoparticles (e.g., wear resistance, and excellent thermal conductivity) as have been discussed in a previous study [41].

The resultant nanofluid is atomized in the MQL system through the applied compressed air, forming a fine mist surrounded with a base cutting fluid film [27]. This mist has the ability to penetrate into the chip-tool interfere zone and forming a tribo-film which helps in absorbing the generated heat and reducing the induced friction. The mentioned characteristics enormously improve the cooling and lubrication properties and retain the cutting tool hardness for a longer time as have been confirmed by Khandekar et al. [40]. In addition to the previous point, using MQL-nanofluid reduces the friction more effectively since the dispersed nanoparticles serve

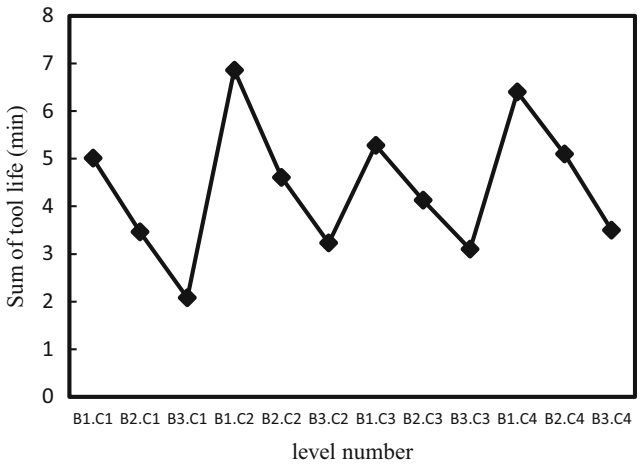

Fig. 5 The interaction effect between the lubrication strategy and cutting speed for the tool life results

Table 6 The coefficient of correlations results

Coolant strategy	Tool life results at feed rate of 0.2 mm/rev	Average surface results at cutting speed of 180 m/min
Dry	− 0.94	0.99
Flood	− 0.91	0.91
MQL	− 0.86	0.97
Nanofluid	− 0.84	0.92

as spacers, eliminating the contact between tool and workpiece [42]. Thus, the MQL-nanofluid offers promising results in terms of tool life improvement (ranging between 15 and 21%) in comparison with tests done using classical MQL. Furthermore, an important point to be considered is that in most machining levels, when 4% gamma-Al_2O_3 nanoparticles are dispersed into vegetable oil, the surface roughness values are decreased.

This improvement is at a value higher than that of pure MQL, except in the case of low-feed-low-speed level where the levels of improvement for both cases are the same as shown in Fig. 3. The findings show that the best surface roughness is 0.625 μm for MQL + 4% gamma-Al_2O_3 nanoparticles at cutting speed of 240 m/min and feed rate of 0.2 mm/rev. The MQL-nanofluid shows improvement in surface quality of 15, 58, and 27.1% in comparison with tests performed at same cutting conditions using MQL, flood, and dry techniques, respectively. The main goal of the nanoparticles is to enhance a heat transfer coefficient and thermal conductivity of the base fluid as well as lubricate the cutting zone during machining process. Because the nanoparticles have a nanometric sizes and spherical shapes, they can be sprayed into the cutting zone, and then be inset into fractured grooves and pores in the cutting zone, as well as between the chips and cutting tool. Then the nanoparticles lubricate the cutting zone which can largely reduce the friction force, and then the cutting forces. The better surface obtained by using nanofluid is probably due to the more effective lubrication and cooling of the tool/workpiece interface and wettability of work material.

Table 4 displays the ANOVA results for the average surface roughness. It shows that the interaction effect between the lubrication strategy and feed rate is the only significant variable at 99% confidence level. Additionally, the interaction effect between the cutting speed and feed rate, and the feed rate effect separately are not significant above 90%; however, they still have acceptable statistical summation about 1.9 and 1.95, respectively (Table 4). The lubrication technique only does not show a significant effect on the resultant surface roughness; however, it still has a promising combined effect with the feed rate as their interaction provides the highest statistical summation. Plot of the interaction effect between the lubrication strategy and cutting feed rate for the measured average surface roughness data shows the optimum level, which provides the lowest summation of average surface roughness as shown in Fig. 4.

It is observed that using MQL with nanofluid and cutting feed rate of 0.2 mm/rev provides the optimal average surface roughness performance (i.e., A1.C4).

Similarly, Table 5 shows ANOVA results for tool life. It is found that the interaction effect between the lubrication strategy and cutting speed is the only significant variables at 95% confidence level. Similar to the surface roughness ANOVA results, the lubrication technique only does not show a significant effect on the resultant tool life; however, it still has a promising combined effect with the feed rate as their interaction provides the highest statistical summation. The plot of the interaction effect between the lubrication strategy and cutting speed for the measured tool life shows the optimum level which provides the highest summation of tool life as shown in Fig. 5. It is observed that cutting speed of 120 m/min with flood or MQL with nanofluid provide the optimal tool life results (i.e., B1.C2 or B1.C4).

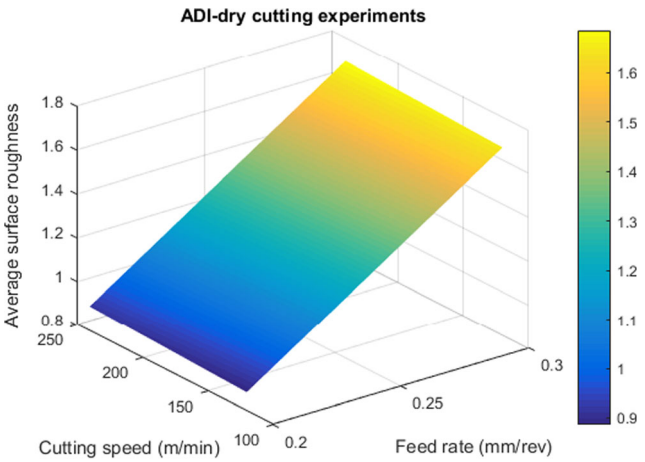

Fig. 6 ADI-dry cutting model for surface roughness results

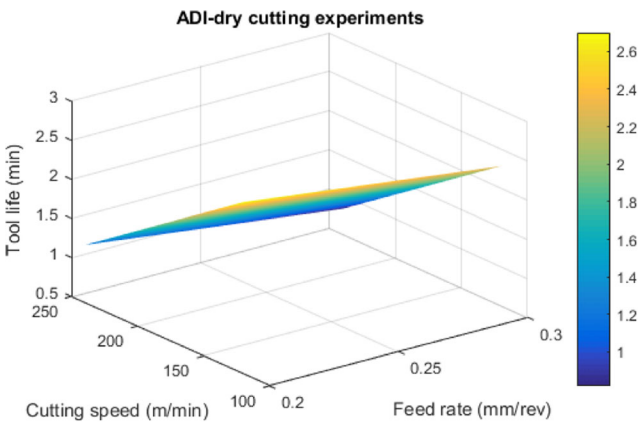

Fig. 7 ADI-dry cutting model for tool life results

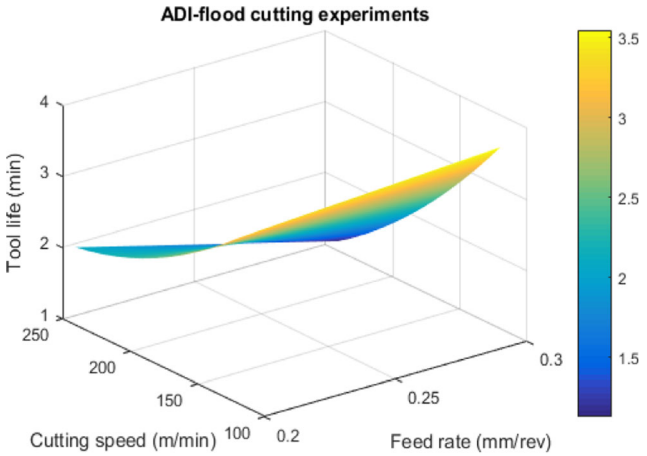

Fig. 8 ADI-flood cutting model for surface roughness results

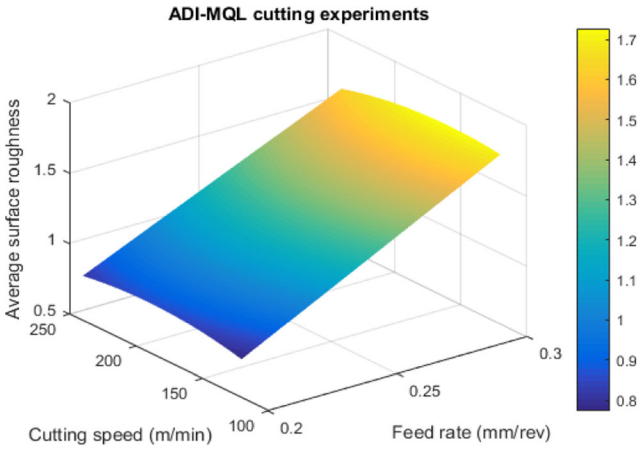

Fig. 10 ADI-MQL cutting model for surface roughness results

Response surface methodology (RSM) is implemented in order to build mathematical models for each lubrication strategy in terms of cutting speed and feed rate to express the predicted average surface roughness and tool life. Therefore, analyzing the influence of the studied independent variables can be demonstrated using this modeling technique as the mathematical model relates the process responses to facilitate the optimization of the process [43].RSM technique has been employed in various machining processes (e.g., milling, turning, and drilling) to study the process variables effects on specific machining quality characteristics (e.g., average surface roughness, cutting forces, tool life) [44–46]. The predicted mathematical models for the average surface roughness using dry, flood, MQL, and MQL with nanofluid are provided in Eqs. 1–4, respectively. Similarly, the tool life models are developed as shown in Eqs. 5–8, respectively. Also, the coefficient of correlations for the all studied cases have been determined and results are listed in Table 6.

In order to validate the proposed mathematical models, average model accuracy is calculated for each case as shown in Eq. 9.

$$\mathrm{Ra)dry} = 7.71f + 0.000025v - 0.6856 \tag{1}$$

$$\mathrm{Ra)}\textit{flood} = 12.945f - 0.0118v - 0.0765fv + 0.000087v^2 + 0.704 \tag{2}$$

$$\mathrm{Ra)MQL} = 10.521f + 0.00849v - 0.0104\,\mathrm{f}v - 0.0000168v^2 - 1.858 \tag{3}$$

$$\mathrm{Ra)}\textit{nanofluid} = 4.18f - 0.0078v + 0.0256fv + 0.28 \tag{4}$$

$$\textit{Tool life)}\mathrm{dry} = -4.166f - 0.0121v + 4.9975 \tag{5}$$

$$\textit{Tool life)}\textit{flood} = 14.11f - 0.012v - 0.0991fv + 0.00006v^2 + 3.455 \tag{6}$$

$$\textit{Tool life)}\mathrm{MQL} = -11.43F - 0.021v + 0.0366fv + 0.0000083v^2 + 6.828 \tag{7}$$

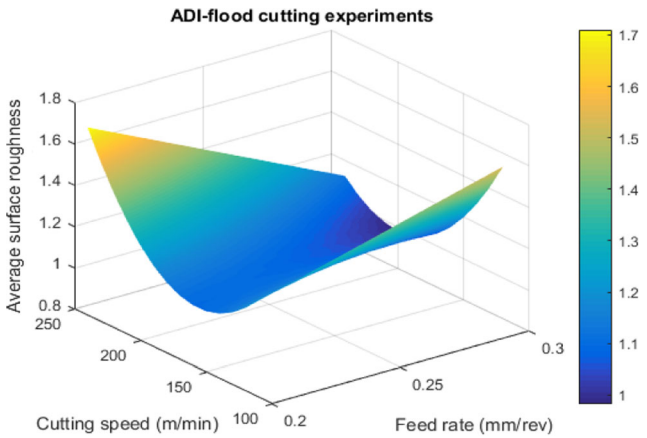

Fig. 9 ADI-flood cutting model for tool life results

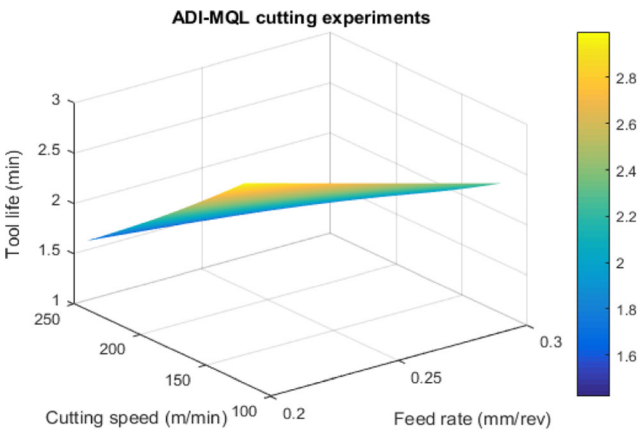

Fig. 11 ADI-MQL cutting model for tool life results

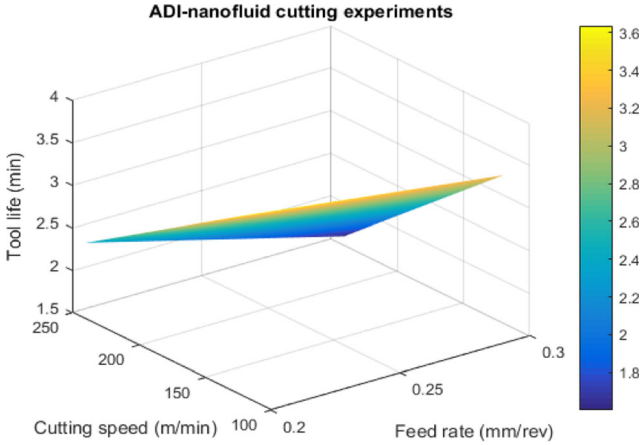

Fig. 12 ADI-nanofluid cutting model for surface roughness results

$$Tool\ life)nanofluid = -0.086f - 0.0037v - 0.033fv + 4.89 \quad (8)$$

$$Average\quad Model\quad accuracy = \frac{\sum_{i=1}^{n} 1 - \frac{\mathrm{Abs}(experimental\ value - predicted\ value)}{experimental\ value}}{n} \quad (9)$$

The mathematical models developed under dry machining technique for tool life, and average surface roughness show average model accuracy about 97.28 and 95.97%, respectively. For MQL strategy, the proposed tool life mathematical model offers 98.78% average accuracy; while the average surface roughness model shows about 90.72%. In terms of flood technique results, the tool life model offers 94.33% average accuracy, and 93.21% average model accuracy is obtained in terms of average surface roughness results. The average accuracy of the nanofluid models are 90.3 and 89.2% for average surface roughness and tool life, respectively. 3-D surface plots for the dry and flood mathematical models are provided as shown in Figs. 6, 7, 8, and 9 while Figs. 10, 11, 12, and 13 show the MQL and nanofluid 3-D surface models.

5 Wear mechanisms analysis

Understanding the tool wear mechanisms is important for optimization of the machining process. From a microstructure perspective, the austenite phase in ADI is thermally stable due to its rich carbon content. It can undergo a strain-induced transformation when the ADI is locally subjected to stress; producing sphere particles of hard martensite which enhances tool wear [47]. All SEM images of worn phases were captured at the end of the cutting tests.

The scanning electron microscope (SEM) images visibly show that the flank wear is the dominated tool wear. Based on the literature [48, 49], the flank wear is essentially caused by abrasion, where the hard particles of the workpiece rub against the tool surface. Furthermore, during chip deformation, particles are pulled out from the contact region of the cutting tool and are taken away by the flowing chips. This act is responsible for tool flank wear and results in shorter tool life. This research evaluates the tool wear at the cutting speed of 120 m/min and feed of 0.2 and 0.3 mm/rev for different coolant methods. The results show that the dominant tool wear observation is the abrasion wear. It was also found that carbon and magnesium particles stacked on the flank face are most likely due to diffusion wear as can be seen from the energy-dispersive X-ray spectroscopy (EDS) image in Fig. 14.

Generally, in all coolant strategies, a few spots of work material adhesion were observed on the insert flank face, which can be attributed to a high cutting temperature at interface zone and the chemical reaction of workpiece materials. Figure 15a presents the cutting edge under dry machining at a cutting speed of 120 m/min and feed of 0.2 mm/rev. It can be observed that adhesion wear with a relatively large abrasion wear appeared along the flank face (red circle). In the case of flood coolant strategy (Fig. 15b), according to SEM observations, less extent of abrasion occurred. An amount of chipping (yellow) is also marked on the cutting edge. As can be seen in Fig. 2, when using the flood strategy, the cutting tool has longer life than when using dry condition; however, it appears more severely damaged than dry in SEM images due to the oxidation, external black layer, resulting from flood coolant Figs. 15b and 16b. The most important SEM observation of the flooding strategy is the appearance of thermal damage. As a chemical reaction wear, thermal damage occurs when chemical compound are formed by reaction of the cutting tool material with

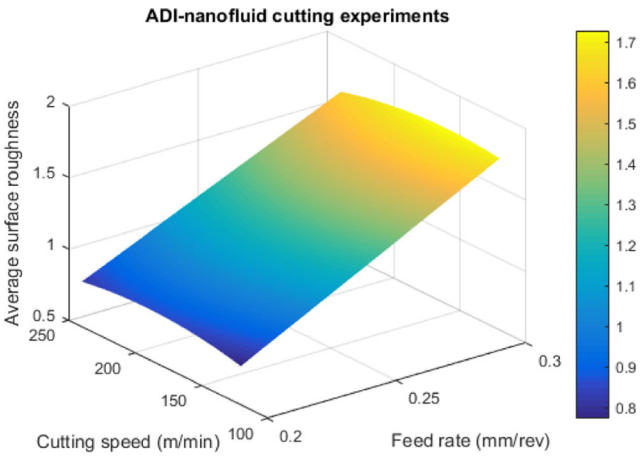

Fig. 13 ADI-nanofluid cutting model for surface roughness results

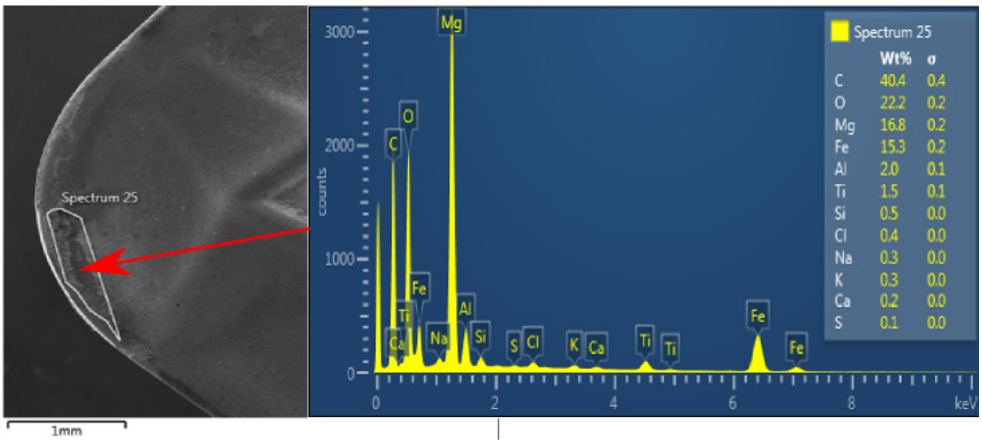

Fig. 14 EDS image for diffusion on tool at dry machining $f = 0.2$ mm/rev and $V = 120$ m/min

the workpiece material at high temperatures in the presence of oxygen [50]. As shown in Fig. 15b, oxidation wear, which appears as a dark area, is marked on the extremity of the tool edge (chip/tool contact region). An oxide layer can act as a barrier against wear at the tool surface; however, it can also accelerate the wear rate. Usually, during the machining process, the air is available in the chip/tool interface area. The presence of air, water (in flood coolant), and high temperature is most likely producing the oxidation wear. Moreover, as seen in Fig. 15c, the vegetable oil MQL yields relatively small abrasion, which seen within the

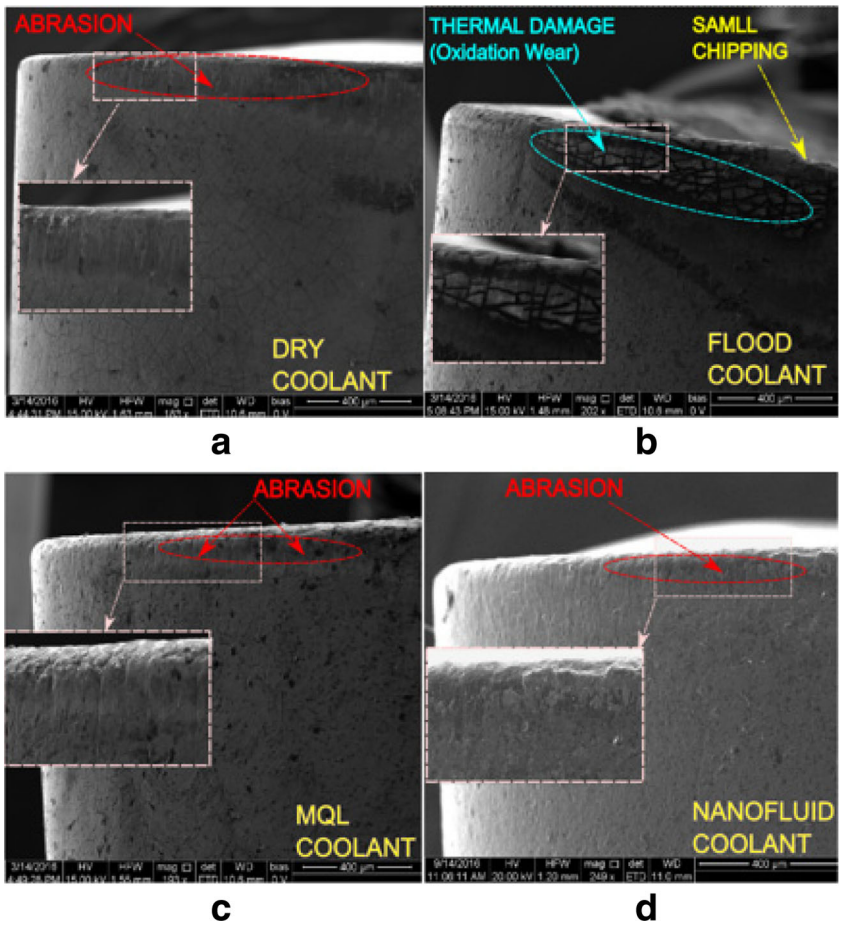

Fig. 15 SEM images of inserts after machining at $V = 120$ m/min and $f = 0.2$ mm/rev under different coolant strategies

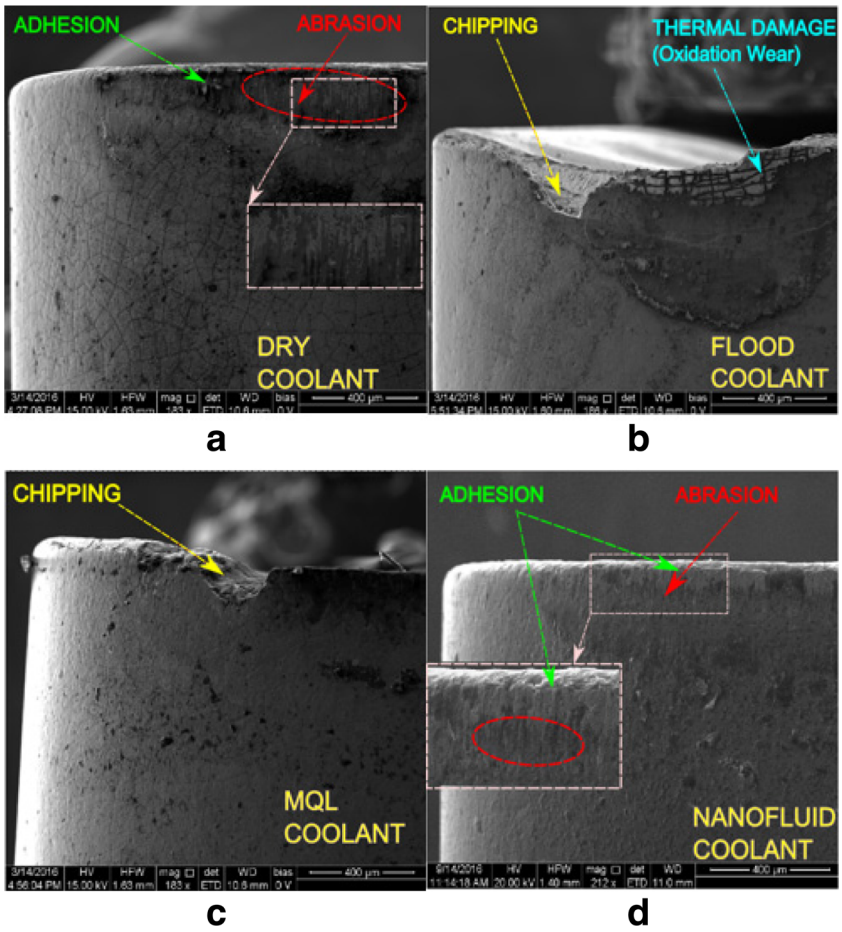

Fig. 16 SEM images of inserts after machining at $V = 120$ m/min and $f = 0.3$ mm/rev under different coolant strategies

red circle. This could be attributed to the lubricant conditions (i.e., forming a fine mist surrounded with a base cutting fluid film) where the vegetable oil reduces the rubbing effect between the hard particles and tool surface, generating less friction and less heat.

The main purpose of dispersed gamma-Al_2O_3 nanoparticles into MQL vegetable oil is to enhance the thermal conductivity and heat transfer coefficient of the coolant. Therefore, in the case of nanofluid coolant (Fig. 15d), less abrasion wear is observed, which is labeled by a red circle. These results indicate that dispersion of gamma- Al_2O_3 nanoparticles into vegetable oil improves the performance of the MQL coolant. Furthermore, Fig. 16a shows the insert cutting edge with abrasive and adhesive wear after dry machining at cutting speed of 120 m/min and feed of 0.3 mm/rev.

A clear chipping is observed in the case of flood coolant as described in Fig. 16b, which could cause a tool failure. The oxidation wear is also observed in the flood strategy at a feed rate of 0.3 mm/rev. From Fig. 16b, it can be seen that a large thermal damage is located very close to the cutting tool edge. As mentioned previously, the presence of oxygen and high temperatures could cause this type of wear mechanism [50]. In the case of MQL, a small chipping is detected as seen in Fig. 16c. Meanwhile, the nanofluid cooling yields less abrasion wear as shown in Fig. 16d. Ultimately, when machining ADI at cutting speed of 120 m/min and feed of 0.3 mm/rev, the extent of flank wear is slightly increased (9–13%) compare to feed of 0.2 mm/rev, and the amount of chipping in the flood method is visibly observed. Increasing the feed rate value mainly leads to increase the induced generated heat, thus resulting into quick thermal softening and rapid cutting edge wear.

6 Conclusions

In this work, machining of ADI grade 2 under four cooling strategies (i.e., flood, dry, MQL, and MQL with nanofluid) was investigated. Three levels of cutting speeds were used: 120, 180, and 240 m/min, and two feeds 0.2 and 0.3 mm/rev. A constant depth of cut of 0.5 mm and length of cut of 50 mm were used for each pass. L24 mixed orthogonal array based on the design of experiments techniques was employed. MQL

with nanofluid shows promising results for both average surface roughness and tool life results.

ANOVA is implemented to study the cutting process variables effects on the measured responses. The interaction effect between the feed rate and cooling strategy is the only significant variable, which affects the average surface roughness. The tool life ANOVA results show that interaction effect between the cutting speed and cooling strategy is the only significant variable. The RSM technique was employed to develop mathematical models for tool life and average surface for each cooling strategy and acceptable models accuracies are observed. Regarding the tool wear mechanisms analysis, the SEM examination revealed that abrasive and adhesive wear mechanisms are dominant modes of tool wear when machining ADI at different cutting parameters, which can be attributed to the hardness and chemical reaction of ADI. Due to a presence of air and elevated temperature at the cutting zone, oxidation wear is noticed when using the flood coolant. Among the four coolant strategies, the nanofluid provided better results at different cutting parameters in terms of tool life and surface quality. The performance of MQL vegetable oil is improved after dispersing 4% gamma- Al_2O_3 nanoparticles, hence, increasing its thermal conductivity is observed.

Also, it can be concluded that using nanofluids can reduce the induced friction at the cutting zone, and consequently that could lead to a significant reduction in the cutting forces. The enhancement in lubricity of nanofluids can be attributed to effect of ball bearing, tribo-film formation, mending, and polishing effects. The better surface obtained by using nanofluid is probably due to the more effective lubrication and cooling of the tool/workpiece interface and wettability of work material.

Acknowledgements The authors acknowledge the support provide by Ontario Centers of Excellence (OCE) and NSERC.

References

1. Namb M, Paulo D (2011) Influence of coolant in machinability of titanium alloy (Ti-6Al-4V). J Surf Eng Mater Adv Technol 1(01):9
2. Trent E, Wright P (1991) Heat in metal cutting. Metal cutting, 3rd edn. Butterworth Heinemann, Oxford, pp 57–85
3. Davim JP (2011) Machining of hard materials. Springer Science & Business Media
4. Davim JP (2008) Machining: fundamentals and recent advances. Springer Science & Business Media
5. Padan D (2012) Microalloying in austempered ductile iron (ADI). AFS Trans 120:1–12
6. Moore D, Rouns T, Rundman K (1985) Structure and mechanical properties of austempered ductile iron. Trans Am Foundry Soc 93: 705–718
7. Dorazil E, Podrabsky T, Svejcar J (1990) Micro-inhomogeneity of low-alloy austempered ductile cast iron matrix. Trans Am Foundry Soc 98:765–774
8. Shih T-S, Lin C-K, Twan H-Z (1997) Mechanical properties of various-section ADIs. in One Hundred First Annual Meeting of the American Foundrymen's Society, Rosemont
9. Shimizu K, Noguchi T, Doi S (1993) Basic study on the erosive wear of austempered ductile iron. Trans Am Foundry Soc 101:225–229
10. Brandenberg K (2001) Successfully machining austempered ductile iron (ADI). Applied Process Inc. Technologies Div.—Livonia, Michigan
11. Datt J, Batra U (2013) Influence of composition and austempering temperature on machinability of austempered ductile iron. World Acad Sci Eng Technol Int J Chem Mol Nucl Mater Metallur Eng 7(2):132–137
12. Incorporated, R.T.I.T (1990) Ductile iron data for design engineers
13. Nofal, A (2013) Advances in the metallurgy and applications of ADI. Journal of Metallurgical Engineering. 2(1)
14. Garin J, Mannheim R (2003) Strain-induced martensite in ADI alloys. J Mater Process Technol 143:347–351
15. Polishetty, A (2011) Machinability and microstructural studies on phase transformations in austempered ductile iron, in PhD Thesis, Auckland University. p. 46–56
16. Smith, Material Science and Engineering Series. 1993, USA: Mc Graw-Hill
17. P. Ashwin, G. Moshe, L. Guy (2010) Wear characteristics of ultrahard cutting tools when machining austempered ductile iron. Int J Mechatron Eng IJMME-IJMNS. 10(1)
18. Kishawy H, Li L, El-Wahab A (2006) Prediction of chip flow direction during machining with self-propelled rotary tools. Int J Mach Tools Manuf 46(12):1680–1688
19. Li L, Kishawy H (2006) A model for cutting forces generated during machining with self-propelled rotary tools. Int J Mach Tools Manuf 46(12):1388–1394
20. Kishawy, H (2002) An experimental evaluation of cutting temperatures during high speed machining of hardened D2 tool steel
21. Davim JP, Figueira L (2007) Machinability evaluation in hard turning of cold work tool steel (D2) with ceramic tools using statistical techniques. Mater Des 28(4):1186–1191
22. Gaitonde V et al (2009) Analysis of machinability during hard turning of cold work tool steel (type: AISI D2). Mater Manuf Process 24(12):1373–1382
23. Gaitonde V et al (2009) Machinability investigations in hard turning of AISI D2 cold work tool steel with conventional and wiper ceramic inserts. Int J Refract Met Hard Mater 27(4):754–763
24. Akdemir, A., et al. (2012) The effect of cutting speed and depth of cut on machinability characteristics of austempered ductile iron. J MAnuf Sci Eng Trans ASME. 134(2)
25. Seker U, Hasitci H (2012) Evaluation of machinability of austempered ductile irons in terms of cutting forces and surface quality. J Mater Process Technol 173:260–268
26. Klocke F, Arft M (2013) High performance turining of austempered ductile iron (ADI) with adapted cutting inserts. Procedia CIRP 8: 129–268
27. Klocke F, Klöpper C, Lung D, Essig C (2007) Fundamental wear mechanisms when machining austemlered ductile iron (ADI). Ann CIRP 56(1):73–76
28. Venugopal K, Paul S, Chattopadhyay A (2007) Tool wear in cryogenic turning of Ti-6Al-4V alloy. Cryogenics 47(1):12–18
29. Cordes S, Hübner F, Schaarschmidt T (2014) Next generation high performance cutting by use of carbon dioxide as cryogenics. Procedia CIRP 14:401–405
30. Stephenson D et al (2014) Rough turning Inconel 750 with supercritical CO 2-based minimum quantity lubrication. J Mater Process Technol 214(3):673–680
31. Nguyen TK, Do I, Kwon P (2012) A tribological study of vegetable oil enhanced by nano-platelets and implication in MQL machining. Int J Precis Eng Manuf 13(7):1077–1083

32. Kitagawa T, Kubo A, Maekawa K (1997) Temperature and wear of cutting tools in high-speed machining of Inconel 718 and Ti-6Al-6V-2Sn. Wear 202(2):142–148
33. AN A (1992) Tool temperatures in interrupted metal cutting. J Eng Ind 114:127
34. Bhowmick S, Alpas AT (2008) Minimum quantity lubrication drilling of aluminium–silicon alloys in water using diamond-like carbon coated drills. Int J Mach Tools Manuf 48(12):1429–1443
35. Bhowmick S, Alpas A (2011) The role of diamond-like carbon coated drills on minimum quantity lubrication drilling of magnesium alloys. Surf Coat Technol 205(23):5302–5311
36. Meena A, El Mansori M (2011) Study of dry and minimum quantity lubrication drilling of novel austempered ductile iron (ADI) for automotive applications. Wear 271(9):2412–2416
37. Klocke, F. and C. Klöpper Machining of ADI. WZL-Laboratory of Machine Tools and Production Engineering, University of Technology, Aachen, Germany https://www.google.ca/url?sa=t&source=web&rct=j&url=http://zanardifonderie.com/wpcontent/uploads/2013/04/Machining-of-ADI.pdf&ved=0ahUKEwjCmqq8ta_WAhUG9IMKHWsrAecQFgg0MAI&usg=AFQjCNGSOP3UZysh_HWnGb4CBK_tKNtdEw Last accessed Sep 3 2017
38. Kim S et al (2006) Effects of nanoparticle deposition on surface wettability influencing boiling heat transfer in nanofluids. Appl Phys Lett 89(15):153107
39. Wang X-Q, Mujumdar AS (2007) Heat transfer characteristics of nanofluids: a review. Int J Therm Sci 46(1):1–19
40. Khandekar S et al (2012) Nano-cutting fluid for enhancement of metal cutting performance. Mater Manuf Process 27(9):963–967
41. Hsieh S-S, Liu H-H, Yeh Y-F (2016) Nanofluids spray heat transfer enhancement. Int J Heat Mass Transf 94:104–118
42. Rahmati B, Sarhan AA, Sayuti M (2014) Morphology of surface generated by end milling AL6061-T6 using molybdenum disulfide (MoS_2) nanolubrication in end milling machining. J Clean Prod 66:685–691
43. Phadke M (1998) Quality engineering using design of experiments, quality control, robust design, and the Taguchi method. Wadsworth, Los Angeles
44. Öktem H, Erzurumlu T, Kurtaran H (2005) Application of response surface methodology in the optimization of cutting conditions for surface roughness. J Mater Process Technol 170(1):11–16
45. Kilickap E (2010) Modeling and optimization of burr height in drilling of Al-7075 using Taguchi method and response surface methodology. Int J Adv Manuf Technol 49(9):911–923
46. Mukherjee I, Ray PK (2006) A review of optimization techniques in metal cutting processes. Comput Ind Eng 50(1):15–34
47. Klocke F et al (2007) Fundamental wear mechanisms when machining austempered ductile iron (ADI). CIRP Ann Manuf Technol 56(1):73–76
48. Odelros, S (2012) Tool wear in titanium machining
49. Byers, J.P (2016) Metalworking fluids. Crc Press
50. De Oliveira, V. and M.T. Dos Santos (2007) Analysis of the cutting tool's wear behavior for turning machining of austempered ductile. in 19th International Congress of Mechanical Engineering. Brasilia